Journal of Engineering Science and Technology
Vol. 2, No. 2 (2007) 126 - 138

THE INFLUENCE OF ROTATING DOMAIN SIZE IN A ROTATING FRAME OF REFERENCE APPROACH FOR SIMULATION OF ROTATING IMPELLER IN A MIXING VESSEL

M. ZADRAVEC*, S. BASIC, M. HRIBERSEK

University of Maribor, Faculty of Mechanical Engineering
Smetanova 17, SI-2000 Maribor, SLOVENIA
*Corresponding Author: matej.zadravec@uni-mb.si

Abstract

This paper presents simulation of rotating impeller in a mixing vessel by means of Computational Fluid Dynamics (CFD). A special emphasis is devoted to the study of influence of the choice of numerical model for simulation of rotation of impeller when mixing a Newtonian fluid in a vessel equipped with Rushton impeller, and operating under turbulent flow conditions. In order to determine the best simulation approach experimental validation of the selected problem is done by means of Particle Image Velocimetry (PIV) system. When using the rotating frame of reference approach, the stirring vessel geometry has to be split into a stationary and rotating part, and the question arises where to position the interface between both regions in order to avoid numerical errors, originating in numerical approximations at the interface. To answer this question, a comparison between the CFD based numerical results and experimental results, was made.

Keywords: Turbulent Flow, Computational Fluid Dynamics, Rotating Frame of Reference, Particle Image Velocimetry.

1. Introduction

Computational Fluid Dynamics has become a powerful tool in simulation of mixing phenomena. Since in mixing operations, the generation of fluid flow is due to the input of mechanical energy in form of rotation of the impeller, the one of very important consideration, when selecting the numerical model, is also the choice of a model, describing impeller rotation. Other models include a turbulence model, multiphase model, rheology model a nd free surface model,

Nomenclatures

b	Baffle width (m)
D	Impeller diameter (m)
h	Impeller distance from bottom of vessel (m)
F	Additional forces (N)
g	Acceleration due to gravity ($m.s^{-2}$)
H	Total liquid depth (m)
k	Turbulent kinetic energy ($m^2.s^{-2}$)
L	Length of blades on impeller (m)
m	Rotating domain height (m)
M	Rotating domain diameter (m)
n	Impeller speed (s^{-1})
p	Pressure ($N.m^{-2}$)
r	Location vector
Re	Reynolds number
s	Clearance of baffle from wall (m)
t	Time (s)
T	Inside diameter of stirred tank (m)
u	Flow velocity in rotating frame ($m.s^{-1}$)
v	Flow velocity ($m.s^{-1}$)
W	Width of blades on impeller (m)
x, y, z	Cartesian coordinates

Greek Symbols

ν	Kinematic viscosity ($m^2.s^{-1}$)
ω	Angular velocity ($rad.s^{-1}$)

among others. In order to keep computational cost low, careful selection of numerical models for mixing should be made.

In the present study, the Rushton turbine, representing a class of radial impellers, was chosen as a model of impeller. This impeller was already extensively studied, experimentally by the use of LDA by Wu and Patterson [1], Ranade and Joshi [2], and Van´t Riet et all [3] among others, studying flow structures in the vicinity of the Rushton impeller. Comparison of CFD based simulation results with PIV obtained experimental results is reported in works of Ranade et all [4] and Khopkar et all [5] among others.

When modeling the impeller motion, the unsteady moving grid techniques, physically the most correct computational models, are expensive to use and therefore not suitable for the majority of engineering computations. The rotating frame of reference technique is a cost effective alternative, suitable for performing steady-state as well as transient simulations, [6]. Within this approach, the region in the vicinity of the impeller is solved using rotating frame of reference and the rest of the computational domain is solved in stationary frame of reference. It is obvious that the rotating region must embed the impeller geometry, the selection of the outer diameter of this region is however left to the skill of the user. Since the flow field, especially viscous stresses, in the vicinity of

the blades is of primary importance in dispersion processes, the width and height of the rotating region can influence the quality of computational results. The aim of the present study was therefore to get an insight into the influence the rotating region dimensions have on the accuracy of computed flow field in the stirred vessel.

2. Experimental Set-Up

A laboratory scale experimental model was set-up for the evaluation of flow field in the mixing vessel. It consisted of cylindrical vessel with flat bottom ($H/T=1$) filled with water. Four side baffles ($s/T=1/12$) were placed in the vessel in close vicinity of the wall, and the six blade Rushton turbine ($D/T=1/3$) was mounted on the shaft. Distance between the bottom and impeller disc was $h/D=1$, and the impeller aspect ratio was set to be $W/D=1/5$. Impeller rotated with constant rotational speed $n=16.67s^{-1}$, resulting in the Reynolds number $Re=D^2n/\nu\approx22\cdot10^3$. Circumferential velocity of the impeller tip was $v_{tip}=(D/2)2\pi n=1.92m/s$. The parameters were identical as in our study [7], which served as a basis for the extended analysis, presented in this paper.

For experimental evaluation of the velocity field the 2D PIV system was used, presented in Fig. 1. Water in the flow region was seeded by silver coated hollow glass spheres with average diameter of $10\mu m$. During the experimentation a planar velocity distribution in narrow region in the vicinity of the impeller tip (Fig. 6) has been visualized. Operational speed of PIV camera was considerably below the rotational speed of impeller. With a view to capture sufficient number of PIV images at different positions of single impeller blade a data acquisition time has been managed in such way that it gave a large series of PIV images. These images are then grouped with regard to instantaneous position of impeller blades allowing for an angular span between the neighboring groups of 15^o. Time between recordings was limited by maximum speed of PIV camera (4 Hz) and had a value of 250 ms. Time between pulses was defined through an optimization procedure and its optimal value for described flow conditions was 200 μs. Instantaneous velocity fields were calculated using an adaptive cross correlation algorithm.

3. Numerical Modelling

For the numerical solution of turbulent mixing of a Newtonian fluid the Reynolds averaged Navier-Stokes equations were selected as a physical model. In our case, the set of governing equations was solved by the use of Ansys-CFX computational code. For accounting the effect of Turbulence was accounted for with the k-ω based Shear Stress Turbulence (SST) [6], as it proved advantageous, compared with the standard k-ε model, for computations of flows with large velocity gradients. For advection scheme the high resolution scheme was used and for time stepping the second order backward Euler scheme was selected. The numerical model included modelling of the free surface flow, and convergence criterion was set with RMS residuals of 10^{-8}.

In order to avoid the use of a moving grid approach the multiple frames of reference technique was used. This means that the inner part of the vessel, containing the rotating impeller, was resolved in rotating frame of reference and

the outer part with baffles, shaft and vessel walls in stationary frame of reference. The stationary frame of reference solves for the absolute velocity v, which is coupled with the relative frame velocity u at the interface between rotating and stationary domain as:

$$\vec{u} = \vec{v} - \omega\vec{r} \tag{1}$$

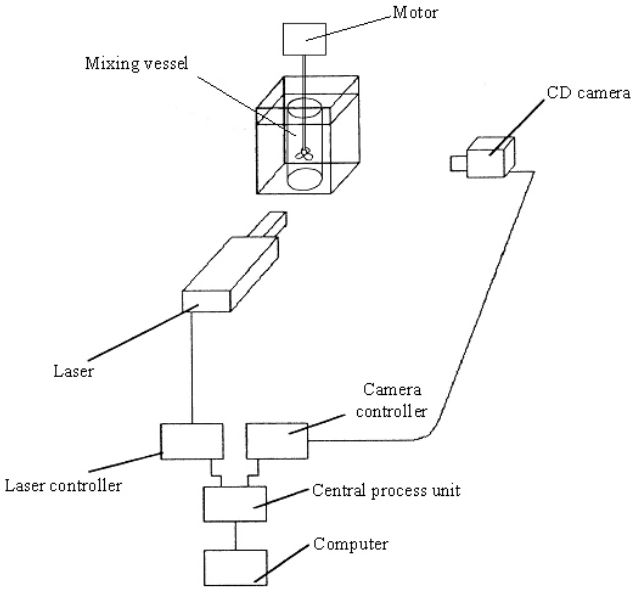

Fig.1. Schematic Diagram of the Experimental Set-Up.

In Eq. 1 ω is a constant angular velocity and $\vec{r}$ is the location vector. In order to simulate the rotation of the inner domain two additional forces in the momentum equation have to be included, the Coriolis (F_{cor}) and centrifugal (F_{cfg}) force:

$$F_i = F_{cor} + F_{cfg} = \underbrace{-2\cdot\omega\times\vec{u}}_{\textit{Coriolis force}} \underbrace{-\omega\times\left(\omega\times\vec{r}\right)}_{\textit{centrifugal force}} \tag{2}$$

Since the domain is decomposed into a rotating and stationary part, appropriate coupling between the two must be made. The coupling was done by transient rotor-stator approach, where relative motion of rotor and stator is done via the interface handling but no actual mesh motion is necessary [6]. In comparison with Frozen-rotor approach, where simulation is performed for one relative position of rotor and stationary part of the vessel, the transient rotor-stator model and simulates movement of rotating parts with regard to other stationary parts of the vessel and is therefore appropriate for transient calculations The transient rotor-stator model requires larger computational times to obtain the

solution, but results in a more physically correct computational solution than the simple frozen rotor model

The rotating region must embed the impeller geometry, but the selection of the outer diameter of this region is left to the skill of the user. In open literature on mixing there are only a few works on this topic, dealing mainly with stationary flows, see Sommerfeld [8]. In order to evaluate the effect of a different size of rotating region a parametric study was conducted, where influence parameters were the dimensions of rotating domain, given in Tab.1 and presented on Fig. 2.

Table.1. Different Dimensions of Rotating Domain.

Model no.	M [m]	m [m]
1	0.0406	0.01132
2	0.0426	0.01332
3	0.0446	0.01532
4	0.0526	0.02332

In order to cut down CPU time and due to the vessel's symmetry only one half of the vessel was modelled (Fig. 3). Mesh used was unstructured and composed of tetrahedrons, prisms and pyramids with inflated boundary on walls. Several computational meshes were checked, and mesh independence tests led to the the mesh with approximately $6 \cdot 10^5$ elements, which was used for all computations.

Regarding the boundary conditions, on the solid walls no slip boundary conditions were prescribed, and on the upper surface of vessel the liquid the free slip boundary condition was used. The shaft was modelled in stationary frame of reference as rotating wall with the same rotational speed ($n=16.67 s^{-1}$) as rotational speed of rotor. All models were solved in transient simulation with time step *0.0025 s* and total time of simulation was *2.25 s*.

4. Results and discussion

In order to perform a detailed comparison of results between simulation and experiment, the experimental measurements were performed first. The measuring plane in the PIV measurements was positioned at the middle plane between two neighbouring baffles Fig. 4.

In Fig. 5 the averaged values of all recordings, in which the angle between impeller tip and the measured plane is 0° (measurement from 52.5° to 7.5°), 15° (measurement from 7.5° to 22.5°), 30° (measurement from 22.5° to 37.5°) and 45° (measurement from 37.5° to 52.5°), are presented. From these results we can see that when the impeller tip is levelled with the measuring plane (Fig. 5 - 0°) the fluid flow slightly deviates from radial direction, but straighten after a distance the flow is rearranged again in the radial direction, perpendicular to the walls of

the vessel. In cases when the experimental results are taken behind the impeller blade (Fig. 5 - 15°, 30°, 45°) we can see the entrainment effect of the fluid behind the impeller blade.

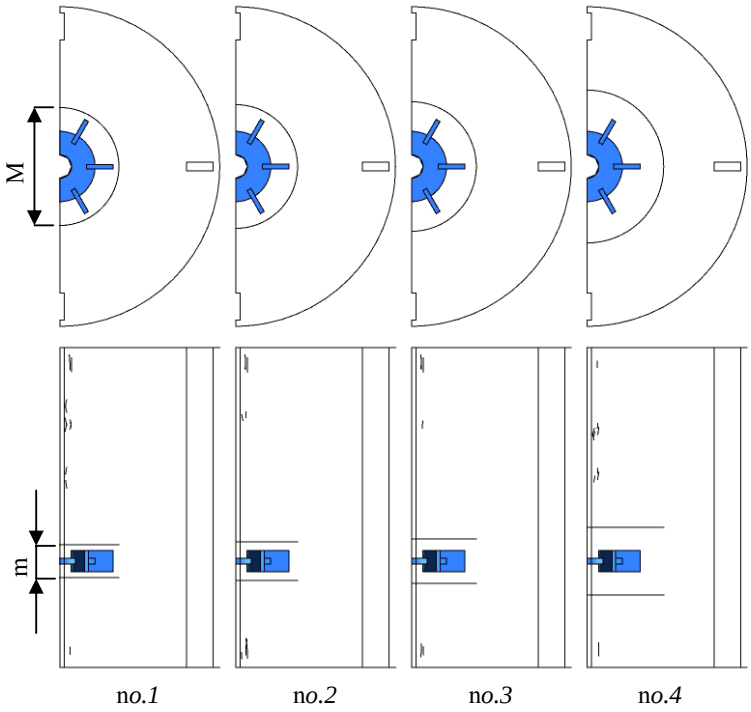

Fig.2. Different Choices for the Rotating Frame of Reference Domain.

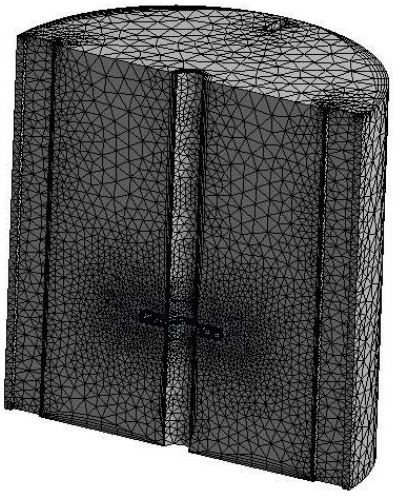

Fig.3. Computational Mesh of the Mixing Vessel.

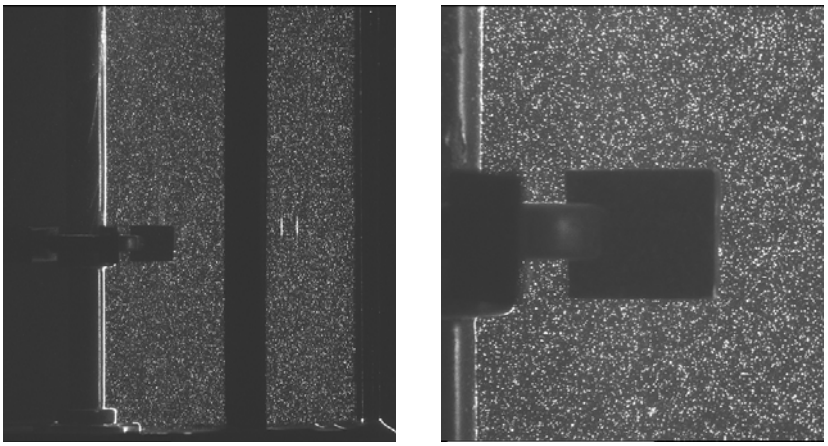

Fig.4. PIV Recordings (Left – the whole vessel, Right – the vicinity of the impeller).

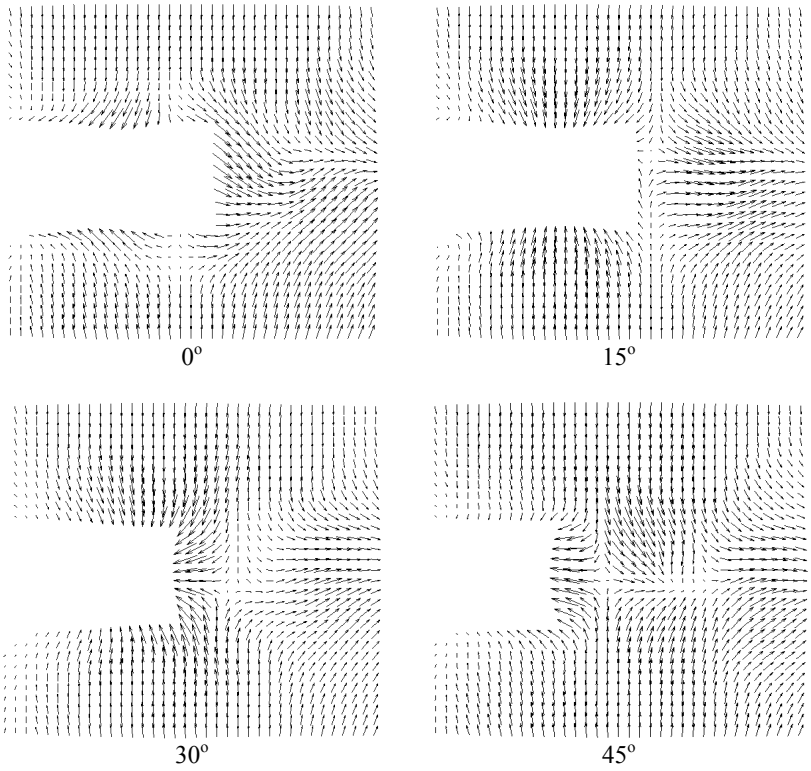

Fig.5. PIV Results for Different Angles between the Impeller Blade and the Measuring Plane.

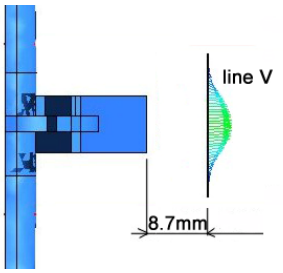

Fig.6. Velocity Result Line.

The PIV velocity fields were used to validate numerical results in the pre-selected lines of comparison, Fig. 6. In general, in the vicinity of the Rushton impeller tip the velocity profile has a form of parabola.

The comparison of the measured and computed velocity profiles is given in Fig. 7 for the line V (Fig. 6) in form of normalized velocities. The angle between the measuring plane and the impeller tip was 0°. The PIV data, used for the purpose of validation, are averaged values of all recordings in which angle between impeller tip and measured plane was 0°. The velocity profiles have the form of parabola as expected. From the results it can be concluded that, in general, the obtained numerical results are in good agreement with measured PIV experimental data, especially regarding that a two-equation turbulence model was used.

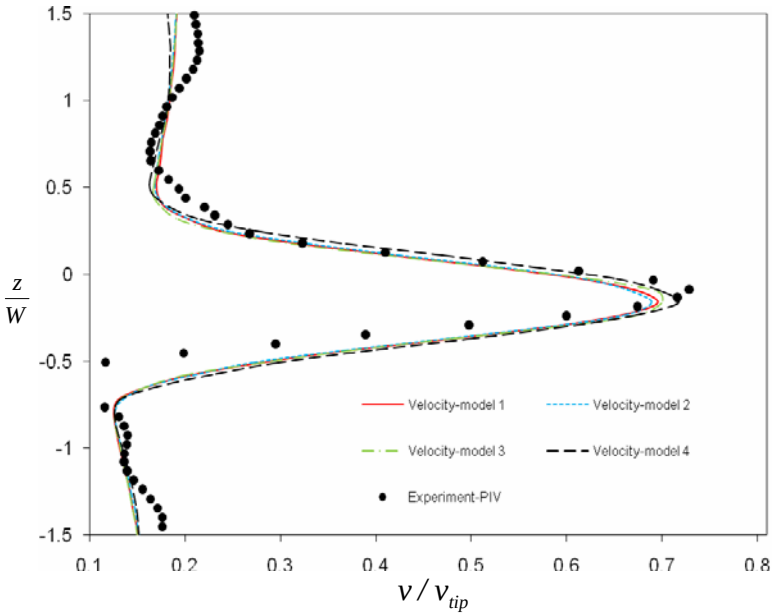

Fig.7. Velocity Profiles Along the Vertical Line V.

When comparing the numerical results obtained with a different size of rotating domain it can be concluded that the numerical model no. 4 is most accurate in following the experimental results. The reason for obtaining different results can be seen from the Fig. 8, where the velocity gradient in the radial direction is shown. When comparing the position, where the flow undergoes transition from accelerating to decelerating flow (x≈0.024) with dimensions of numerical models, it is evident, that the first two models have dimensions smaller than the transition point, only the largest model (model no.4) exceeds this point with its radius of 0.0263.

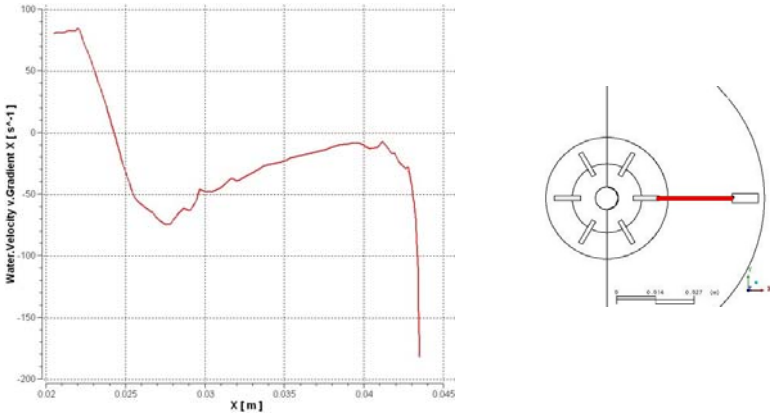

Fig.8. Velocity Gradient in Radial Direction (left), Position of the Line (right).

When comparing numerical results obtained with different sizes of rotating domain it can be concluded that the numerical model with the largest rotating domain (model no.4) is the most accurate in following the experimental results. The boundary between inner and outer numerical domain clearly has a certain damping effect on flow field, which can be observed also from Figs. 9-12.

The upper picture in Fig. 9 presents the surface streamlines on the middle plane of the impeller. Streamline pattern is as expected and the same is valid for the vortices behind the baffles. In lower part of Fig. 9 we can see that in the vessel there are two major vortices, one is under and one above the impeller, what is a typical behaviour in a vessel equipped with the Rushton impeller. Fig. 10 presents contours of velocity. The highest velocities are behind the impeller blade and in the middle between the baffle and the wall. The turbulent kinetic energy and the total pressure are presented on Fig. 11 and Fig. 12.

From the presented results it can be concluded, that one should not choose arbitrary the size of the rotating domain in case of using multiple frames of reference approaches. The position of the interface should avoid intersecting the flow region, where the flow makes a transition from accelerating to deccelerating flow after being pumped by the action of the impeller.

5. Conclusions

Numerical simulations of process devices are becoming more and more important, especially with the development of powerful simulation tools. However, skills of the human modeller are still an important part in obtaining high quality results. In our research work, we have shown on the example of numerical simulation of mixing in a Rushton agitated mixing vessel, that also the choice of the model accounting for the rotation of the impeller has its influence on the numerical results. In the case of a multiple frames of reference results, we found that by enlarging the dimension of the rotating part, the influence of numerical errors due to interpolation inaccuracies in transferring the results between both domains is decreased, hence resulting in more accurate results.

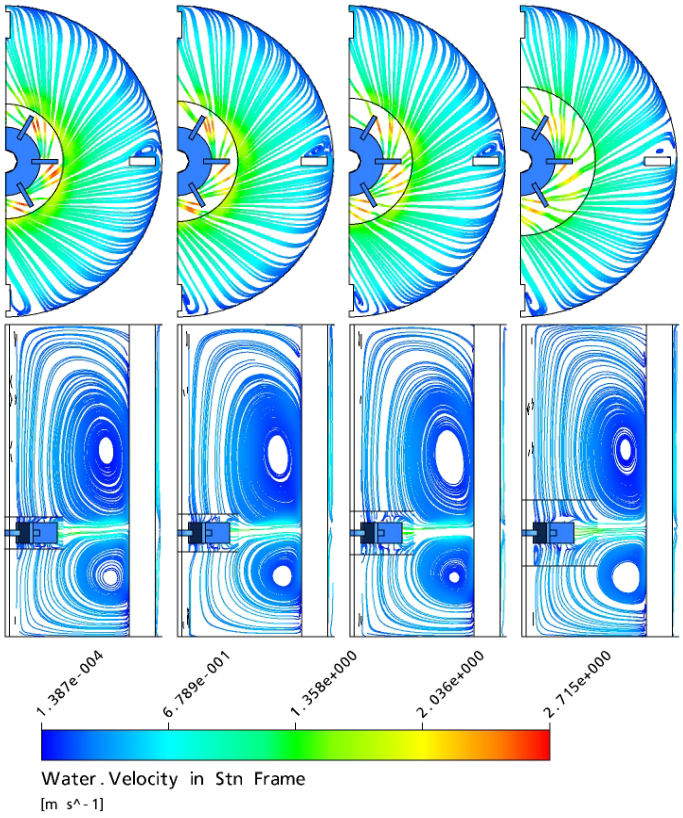

Fig.9. Velocity Streamlines Distribution.

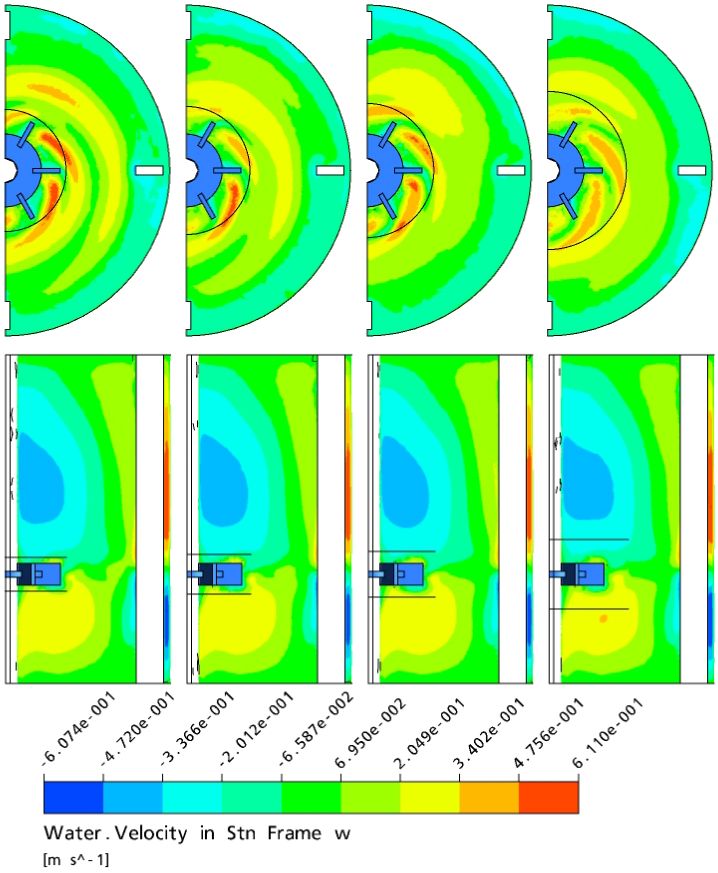

Fig.10. Velocity Contours Distribution.

References

1. Wu, H., & Patterson, G.K. (1989). Laser-Doppler Measurements of Turbulent Flow Parameters in A Stirred Tank. *Chem. Eng. Sci.*, 44, 2207-2221.
2. Ranade, V.V., & Joshi, J.B. (1990). Flow Generated by A Disc Turbine (Part I, Part II). *Trans. IChemE.*, 68: Part A, 19-50.
3. Van`t Riet, K., & Smith John, M. (1975). The Trailing Vortex System Produced by Rushton Turbine Agitators. *Chem. Eng. Sci.*, 30, 1093-1105.
4. Ranade, V. V., Perrard, M., Le Sauze, N., Xuereb, C., & Bertrand, J. (2001). Trailing Vortices of Rushton Turbine: PIV Measurements and CFD Simulations with Snapshot Aproach. *Trans IChemE*, 79: Part A, 3-12.
5. Khopkar, A., Aubin, J., Rubio-Atoche, C., Xuereb, C., Le Sauze, N., Bertrand, J., & Ranade, V. V. (2004). Flow Generated by Radial Flow

Impellers: PIV Measurements and CFD Simulations. *International Journal of Chemical Reactor Engineering*, 2: A18, 1-17.
6. Ansys-CFX. (2005). *ANSYS CFX-Solver, Release 10.0: Modelling.*
7. Zadravec, M., Basic, S., & Hribersek, M. (2006). Evaluation of the Effect of Different Size of Rotating Impeller Region in CFD. In *Proc. 12th European conference on mixing*. Bologna, Italy, 471-478.
8. Sommerfeld, M., & Decker, S. (2004). State of the art and future trends in CFD simulation of stirred vessel hydrodynamics. *Chem. Eng. Technol*., 27 (3), 215-224.

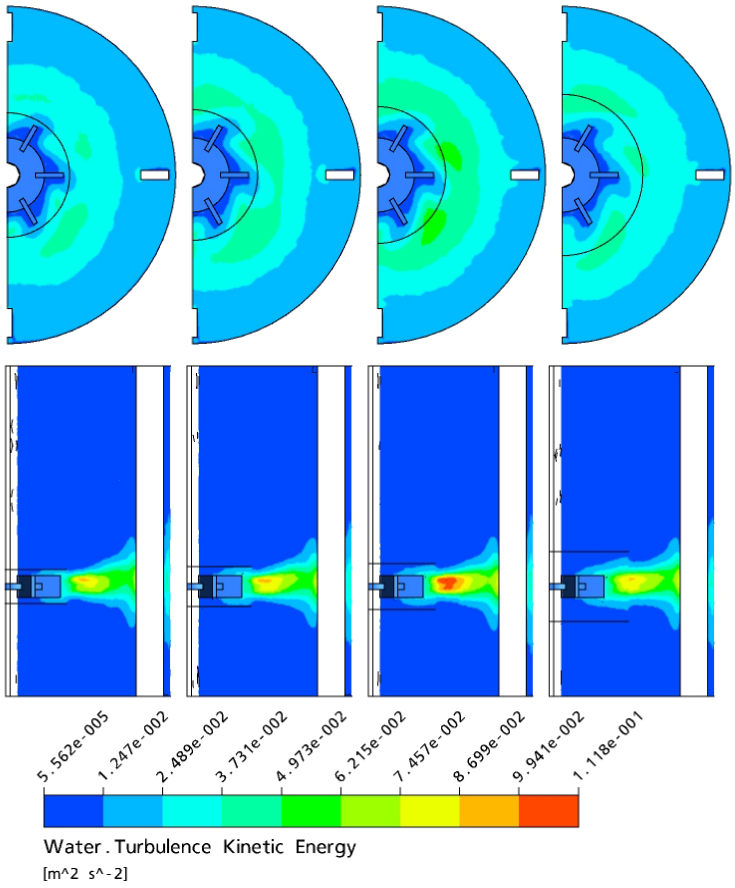

Fig.11. Tturbulence Kinetic Energy Distribution.

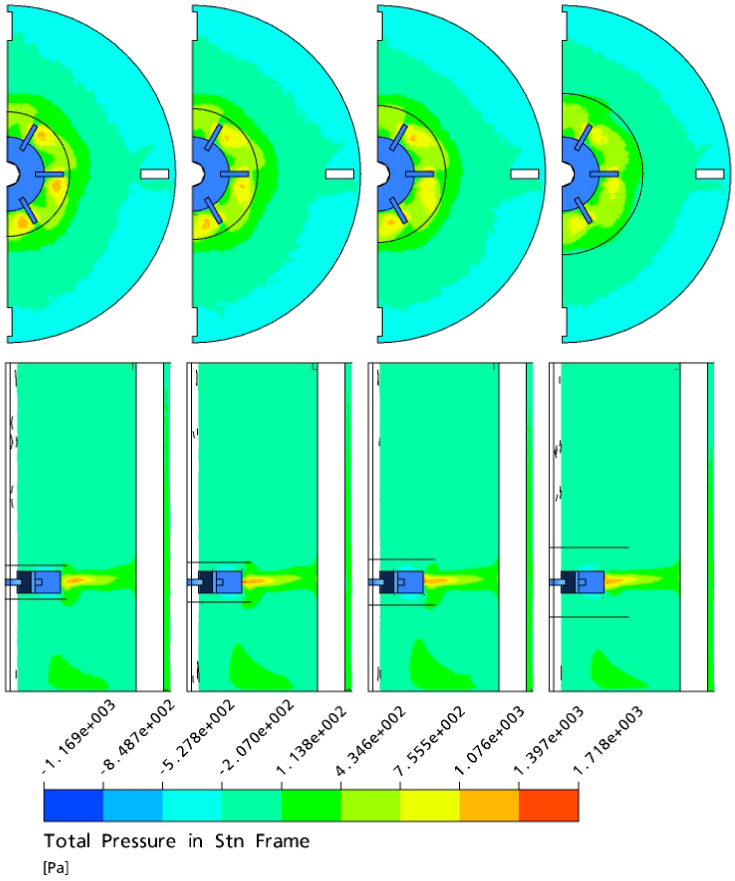

Fig.12. Total Pressure Distribution.